TISSUE ENGINEERING: Part A
Volume 22, Numbers 5 and 6, 2016

DOI: 10.1089/ten.tea.2015.0545

termis
Tissue Engineering
& Regenerative Medicine
International Society

ORIGINAL ARTICLE

Effects of Dexamethasone on Satellite Cells and Tissue Engineered Skeletal Muscle Units

Brian C. Syverud, MS,[1] Keith W. VanDusen, MS,[2] and Lisa M. Larkin, PhD[1,2]

Tissue engineered skeletal muscle has potential for application as a graft source for repairing soft tissue injuries, a model for testing pharmaceuticals, and a biomechanical actuator system for soft robots. However, engineered muscle to date has not produced forces comparable to native muscle, limiting its potential for repair and for use as an *in vitro* model for pharmaceutical testing. In this study, we examined the trophic effects of dexamethasone (DEX), a glucocorticoid that stimulates myoblast differentiation and fusion into myotubes, on our tissue engineered three-dimensional skeletal muscle units (SMUs). Using our established SMU fabrication protocol, muscle isolates were cultured with three experimental DEX concentrations (5, 10, and 25 nM) and compared to untreated controls. Following seeding onto a laminin-coated Sylgard substrate, the administration of DEX was initiated on day 0 or day 6 in growth medium or on day 9 after the switch to differentiation medium and was sustained until the completion of SMU fabrication. During this process, total cell proliferation was measured with a BrdU assay, and myogenesis and structural advancement of muscle cells were observed through immunostaining for MyoD, myogenin, desmin, and α-actinin. After SMU formation, isometric tetanic force production was measured to quantify function. The histological and functional assessment of the SMU showed that the administration of 10 nM DEX beginning on either day 0 or day 6 yielded optimal SMUs. These optimized SMUs exhibited formation of advanced sarcomeric structure and significant increases in myotube diameter and myotube fusion index, compared with untreated controls. Additionally, the optimized SMUs matured functionally, as indicated by a fivefold rise in force production. In conclusion, we have demonstrated that the addition of DEX to our process of engineering skeletal muscle tissue improves myogenesis, advances muscle structure, and increases force production in the resulting SMUs.

Introduction

Potential applications for engineered skeletal muscle include implantation as a graft material for repair of traumatic damage,[1,2] recapitulation of native development, regeneration for detailed physiological study or pharmaceutical testing,[3] and use as biomechanical actuators.[4,5] In each case, recreating the complex function and structure of skeletal muscle *in vivo* is a challenging, but essential, consideration. Engineered tissues to date, however, have been characterized by a neonatal phenotype in terms of force production and structural maturity.[6,7] Following sufficient recovery time, engineered skeletal muscles implanted into an *in vivo* regenerative environment have advanced toward the adult phenotype,[8,9] and several studies have attempted to utilize key chemical and mechanical stimuli to improve the maturity of these engineered muscles *in vitro*.[10,11]

Tissue engineers have used the influence of such growth factors on myogenesis to direct techniques for engineering skeletal muscle. Current tissue engineering techniques utilize scaffold materials, ranging from acellularized tissues[12,13] to collagen and fibrin hydrogels,[3,6,14] or opt for a scaffold-free approach[7,9,15] to support development of extracellular matrix (ECM) for subsequent muscle tissue. The ultimate success of these approaches depends on the *in vitro* culture of isolated primary muscle precursor cells. A common technique in cultivation of these myogenic cells begins with an initial proliferation phase, allowing cells to expand sufficiently, followed by induction of differentiation and fusion into myotubes.[16] Use of media with high serum content is generally accepted to promote the initial proliferation phase while delaying the onset of differentiation, potentially due to the presence of a variety of growth factors.[17] Drastic reduction in media serum content subsequently triggers satellite cell differentiation, possibly due to the removal of essential mitogenic components. Because of variations in the activity and concentration of growth factors between lots of commercially available serum, and the consequent variability in

Departments of [1]Biomedical Engineering and [2]Molecular and Integrated Physiology, University of Michigan, Ann Arbor, Michigan.

satellite cell induction and proliferation, an optimum serum formulation and the identity of these mitogenic components has yet to be fully defined.[18] By understanding the essential growth factors and supplementing media with the appropriate doses, tissue engineers can maximize the myogenic potential of satellite cells when engineering skeletal muscle.

The synthetic glucocorticoid dexamethasone (DEX) has previously been studied due to its profound effects on muscle *in vivo* and on satellite cell cultures *in vitro*, but its application in skeletal muscle tissue engineering has yet to be evaluated. In a clinical setting, DEX is typically used for its anti-inflammatory or immunosuppressant activity to treat several rheumatologic and skin diseases, because it is 25 times more potent than endogenous cortisol.[19] In skeletal muscle specifically, exogenously delivered DEX has a variety of effects depending on the timing and dosage of the administration. DEX induces atrophy in adult human skeletal muscle when supplied orally in 4 mg doses, $\sim$10 times greater than endogenous cortisol levels.[20,21] This atrophic effect has been linked to upregulation of the myostatin promoter and inhibition of IGF-1 expression.[20,22] In contrast, the administration of 5–25 nM DEX has improved myogenesis *in vitro* by enhancing differentiation and myotube fusion of myogenic murine cells, potentially through its induction of dysferlin, a calcium-binding transmembrane protein thought to play a key role in both myogenesis and membrane repair.[23] Similar studies have demonstrated that DEX can inhibit protein synthesis and myoblast proliferation *in vitro*,[24] however, reinforcing the need for careful timing of addition to culture.

Recent research from our lab has focused on optimizing and testing skeletal muscle units (SMUs), cylindrical tissue constructs featuring muscle fabricated from monolayers of primary fibroblasts and contractile myotubes.[9] The articles referenced above regarding DEX activity *in vitro* describe its effects on the immortal C2C12 mouse myoblast cell line in two-dimensional culture, rather than the primary cell population and functional three-dimensional (3D) constructs used in our SMU experiments. We hypothesized that exposing the heterogeneous pool of satellite cells and fibroblasts used for SMU fabrication to different doses of DEX at several time points may yield an optimal combination for improving myogenesis and ultimately maximizing *in vitro* development of our engineered skeletal muscle. Thus, the purpose of this study was to examine the potential of the steroid DEX as a growth factor for skeletal muscle tissue engineering.

Materials and Methods

Animal care

Tissue engineering studies were conducted using soleus muscles and bone marrow from 145 to 155 g female Fischer 344 rats, obtained from Charles River Laboratories, Inc. (Wilmington, MA) and Harlan Laboratories (Haslett, MI). All animals were acclimated to colony conditions for 1 week before any procedure. Animals were fed Purina Rodent Chow 5001 and water *ad libitum.* All surgical procedures were performed in an aseptic environment, with animals in a deep plane of anesthesia induced by intraperitoneal injections of sodium pentobarbital (65 mg/kg). Supplemental doses of pentobarbital were administered as required to maintain an adequate depth of anesthesia. All animal care and animal surgery procedures were in accordance with *The Guide for Care and Use of Laboratory Animals*,[25] and the protocol was approved by the University Committee for the Use and Care of Animals.

SMU formation and DEX addition

SMUs were fabricated in individual coated 60 mm polystyrene plates (BD Falcon, Franklin Lakes, NJ), and immunocytochemistry (ICC) was performed on 35 mm plates as described previously.[7,9,26] Briefly, a substrate of Sylgard (type 184 silicon elastomer; Dow Chemical Corp., Midland, MI) was initially cured onto each plate, followed by coating with laminin (Natural Mouse Laminin; Cat. No. 23017-015; Gibco BRL, Carlsbad, CA) at 1 mg/cm^2. The cell isolation mixture was plated in muscle growth medium (MGM) at a density of 600,000 cells per 60 mm plate and 150,000 cells per 35 mm plate. MGM contained 30 mL F-12 Kaighn's modification nutrient mixture (Cat. No. 21127-022; Gibco BRL), 12.5 mL Dulbecco's modified Eagle's medium (DMEM; Cat. No. 11995-065; Gibco BRL), 7.5 mL fetal bovine serum (FBS; Cat. No. 10437-028; Gibco BRL), 2.4 ng/mL basic fibroblast growth factor (Cat. No. 100-18B; Peprotech, Rocky Hill, NJ), and 0.5 mL antibiotic-antimycotic (ABAM; Cat. No. 15240-062; Gibco BRL).

After the initial plating, cells were left undisturbed for 4 days and subsequently fed MGM every 2 days until becoming fully confluent with elongating myotubes forming a network across the base of the plate. At this point, 5 mm tissue-engineered bone-tendon anchors were pinned onto the cell monolayers 2.5 cm apart, and the media was switched to muscle differentiation medium (MDM). MDM was composed of 35 mL M199 (Cat. No. 11150-059; Gibco BRL), 11.5 mL DMEM, 3 mL FBS, 50 μL insulin-transferrin selenium-X (Cat. No. I1884; Sigma-Aldrich, St. Louis, MO), 0.5 mL ABAM, and 36.2 μL 50 mM ascorbic acid 2-phosphate. After approximately a week on MDM, resupplied every other day, the monolayers delaminated from the plates, rolling into cylindrical muscle constructs, held at length by the engineered bone anchors. During this SMU formation process, described in Figure 1, DEX was added to the media beginning at three different time points: initial plating (day 0), 6 days after initial plating (day 6), and 2 days after the switch to MDM (day 9). These three time points were chosen to evaluate the efficacy of DEX in controlling isolated cell proliferation, differentiation, and maturation of the delaminating monolayer and subsequent 3D SMU, respectively. After the first addition, supplemental doses of DEX were added with each media change. Three experimental doses were supplied (5, 10, and 25 nM), with untreated plates as controls.

SMU contractile measurements

Contractile properties of SMUs ($n=6$) from each experimental group were measured following roll-up into cylindrical form. The protocol for measuring contractility of engineered muscle constructs has been described previously.[27,28] Briefly, the pin on one end of the SMU was raised from the Sylgard and attached to a force transducer. Platinum wire electrodes were placed along either side of the SMU for field stimulation. The temperature of the construct was maintained at 37°C, using a heated aluminum platform. Passive force was measured as the average baseline force

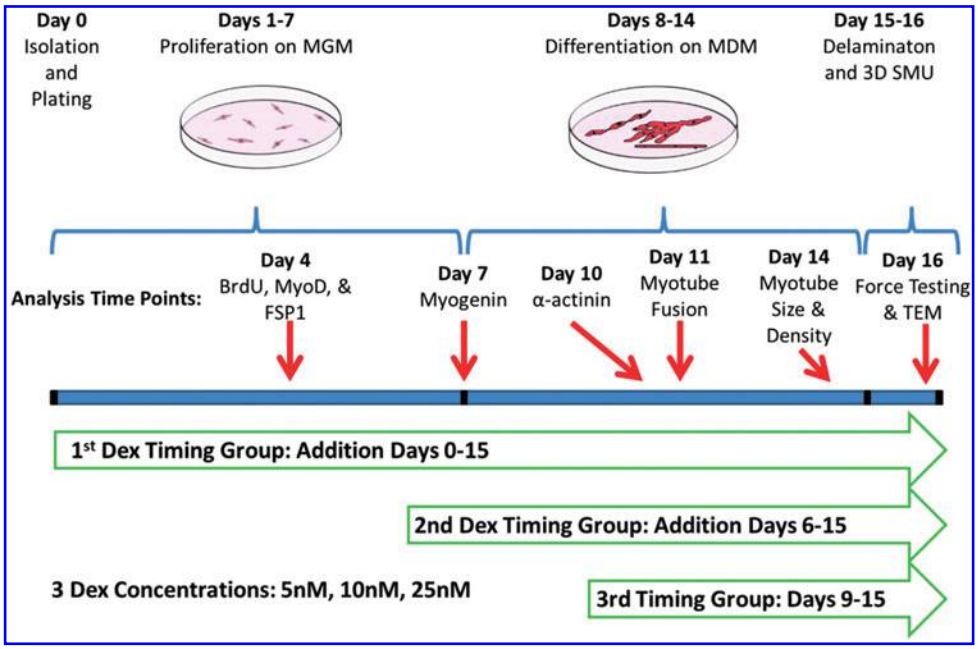

FIG. 1. Experimental timeline. Addition of DEX was initiated at three time points: on day 0 to study effects on proliferation, on day 6 to study effects on late proliferation and differentiation, and on day 9 to study effects on structural maturation. During this SMU fabrication process, subsets of the developing plates were analyzed for expression of BrdU, MyoD, FSP1, myogenin, and α-actinin as listed above. Additionally, myotube fusion and myotube size and density were measured in the developing muscle monolayers. Finally, the 3D SMUs were assessed for force production in response to electrical stimulation and for structural development with TEM. 3D, three-dimensional; DEX, dexamethasone; FSP1, fibroblast-specific protein 1; MDM, muscle differentiation medium; MGM, muscle growth medium; SMU, skeletal muscle unit; TEM, transmission electron microscope.

produced before the onset of stimulation. Twitch contractions were elicited using a single 2.5 ms pulse at 10, 30, 60, and 90 mA, whereas tetanic force was determined using a 1 s train of 2.5 ms pulses at 90 mA and 10, 20, 40, 60, and 80 Hz. Data files for each peak twitch force and peak tetanic force trace were recorded and subsequently analyzed using LabVIEW 2012.

Immunocytochemical analysis

During SMU fabrication, a subset of the plates from each experimental group was fixed in 20°C methanol for 10 min and set aside for ICC. The plates were submerged for 15 min in 0.1% Triton X-100 (Cat. No. T8787; Sigma) in DPBS (PBST) and blocked with PBST containing 3% bovine serum albumin (PBST-S; Cat. No. A2153; Sigma) at room temperature. The sections were then incubated overnight at 4°C with the primary antibodies diluted in PBST-S. Immunofluorescent staining with specific antibodies was performed to detect the presence of BrdU (biotin conjugated sheep polyclonal antibody; Cat. No. ab2284; Abcam, Cambridge, MA), MyoD (mouse monoclonal antibody 1:100 dilution; Cat. No. 554130; BD Biosciences, San Jose, CA), fibroblast-specific protein 1 (FSP1; rabbit polyclonal antibody 1:100 dilution; Cat. No. ab27957; Abcam), myogenin (rabbit polyclonal antibody 1:50 dilution; Cat. No. sc-576; Santa Cruz Biotechnology, Dallas, TX), desmin (mouse monoclonal antibody 1:20 dilution; Cat. No. D3; Developmental Studies Hybridoma Bank, Iowa City, IA), and α-actinin (mouse monoclonal antibody 1:200 dilution; Cat. No. A7752; Sigma). Plates stained with antibodies for BrdU had previously been incubated for 24 h with a BrdU labeling reagent (Cat. No. 00-0103; Life Technologies, Carlsbad, California) in the culture media. Following three washes in PBST, samples were incubated in 1:500 dilutions of Alexa Fluor anti-mouse, anti-rabbit, or streptavidin secondary antibodies (Life Technologies) for 3 h at room temperature. Following three washes in PBST, samples were preserved in Prolong Gold with DAPI (Cat. No. P36935; Life Technologies) and cover slipped. The samples were examined and photographed with a Leica Inverted microscope, and images were analyzed using the Image J software package.

For ICC analysis, plates ($n=5$) from each experimental group were fixed and stained (on day 4 for BrdU, MyoD, and FSP1; day 7 for myogenin; and day 11 for desmin). From each plate, 10 areas were randomly selected and imaged, and the number of positively stained nuclei in each image was counted. To calculate myotube fusion index from the desmin images, the number of nuclei associated with a desmin-positive myotube was divided by the total number of nuclei.

Myotube size and density analysis

On day 14 after initial plating of satellite cells, light micrographs of the developing monolayers in each experimental group were captured and analyzed. Specifically, five areas from each 60 mm plate ($n=8$) were randomly selected and imaged. Every myotube from these images was then measured in ImageJ to determine its size and the overall density of the myotube network.

Transmission electron microscopy analysis

Following measures of mechanical function, SMUs were fixed overnight at room temperature in 0.1 M phosphate buffer (Cat. No. S369-500; Fisher Scientific, Pittsburgh, PA) containing 2.5% glutaraldehyde (Cat. No. 16210; Electron Microscopy Sciences, Hatfield, PA), postfixed at 4°C for 1 h in 0.1 M phosphate buffer containing 1% osmium tetroxide (Cat. No. 19150; Electron Microscopy Sciences), and polymerized in Embed 812 resin (Cat. No. 14900; Electron Microscopy Sciences) at 60°C for 24 h. Ultra-thin 70 nm sections were then cut and stained with uranyl acetate (Cat. No. 22400; Electron Microscopy Sciences) and lead citrate (Cat. Nos. 17900 and 21140; Electron Microscopy Sciences) and imaged using a JEOL JEM-1400Plus transmission electron microscope (TEM).

Statistical analysis

Values are presented as mean ± SE. Measurements of significant differences between means were performed using R software. Means were compared using either one-way or two-way ANOVA tests with Tukey *post hoc* comparisons. Differences were considered significant at $p < 0.05$.

Results

Effects of DEX on proliferation of satellite cells

To assess the influence of DEX on the induction and proliferation of isolated myogenic satellite cells, DEX was added at the time of plating (day 0). ICC analysis of cells expressing BrdU, a synthetic nucleoside analog of thymine, was used on day 4 to identify proliferating cells,[29] and expression of MyoD and FSP1 was examined simultaneously to identify myogenic cells and matrix-secreting fibroblasts, respectively (Fig. 2). From the analysis of BrdU and MyoD co-staining, a dose-dependent response to DEX treatment was evident, with the density of proliferating myogenic nuclei increasing with increasing DEX concentration. Following addition of 10 and 25 nM DEX, a statistically significant increase in $MyoD^+$ cell proliferation relative to No DEX controls was observed ($p = 0.012$ and 0.003, respectively). Addition of 5 nM DEX exhibited no difference from controls and resulted in significantly fewer proliferating $MyoD^+$ cells than the 10 and 25 nM DEX doses ($p = 0.037$ and 0.009, respectively). Similarly, ICC analysis for both BrdU and FSP1 showed that the administration of DEX on day 0 led to a decrease in the number of proliferating $FSP1^+$ cells. This decrease in $FSP1^+$ cells was significant following 10 and 25 nM DEX addition, relative to untreated controls ($p = 0.002$ and 0.004, respectively). Administration of 5 nM DEX indicated no difference in $FSP1^+$ cells from No DEX controls. In comparison to the 10 and 25 nM concentrations, however, 5 nM DEX yielded significantly decreased proliferation of $FSP1^+$ cells ($p = 0.004$ and 0.005, respectively). Thus, the results for MyoD and FSP1 expression in proliferating cells demonstrate that the influence of 10 and 25 nM DEX on early growth of heterogeneous muscle isolates was twofold: improved proliferation of cells in the myogenic lineage and decreased proliferation of non-myogenic fibroblasts.

DEX induction of muscle cell differentiation and myotube fusion

ICC analysis of myogenin expression was used as an indicator of myoblast differentiation into myotubes on day 7 of the experiment.[30] A dose-dependent increase in myogenin-positive cell density was observed in response to DEX treatment, independent of the timing of its addition (Fig. 3A). Groups receiving 5 nM DEX showed no difference from No DEX controls, whereas 10 nM addition significantly

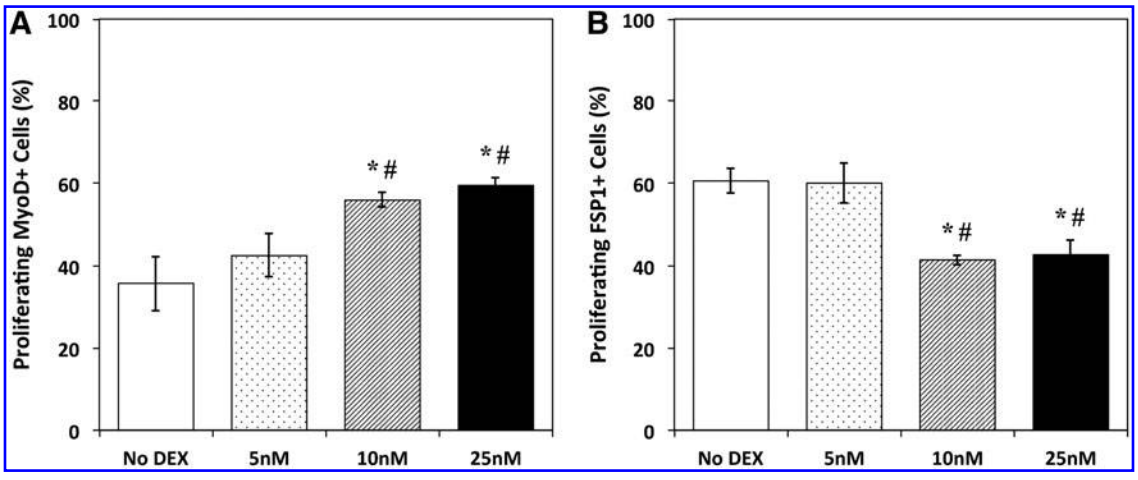

FIG. 2. Myogenic and fibroblast cell proliferation following DEX addition. **(A)** With DEX addition on the day of initial seeding (D0), the percentage of proliferating cells expressing MyoD followed an increasing trend with increasing DEX concentration, as indicated by BrdU and MyoD co-staining on day 4. A statistically significant increase in proliferation ($p = 0.012$ for 10 nM, $p = 0.003$ for 25 nM) was observed when comparing the higher concentrations of DEX (10 and 25 nM) to untreated controls (No DEX). **(B)** ICC analysis for BrdU and FSP1 on day 4 showed a decrease in the percentage of proliferating cells expressing FSP following DEX addition. In response to administration of 10 and 25 nM DEX, the number of proliferating cells expressing FSP1 significantly decreased relative to No DEX controls ($p = 0.002$ and 0.004, respectively). Error bars indicate mean ± standard error. *Indicates statistical difference from control, #from 5 nM DEX. ICC, immunocytochemistry.

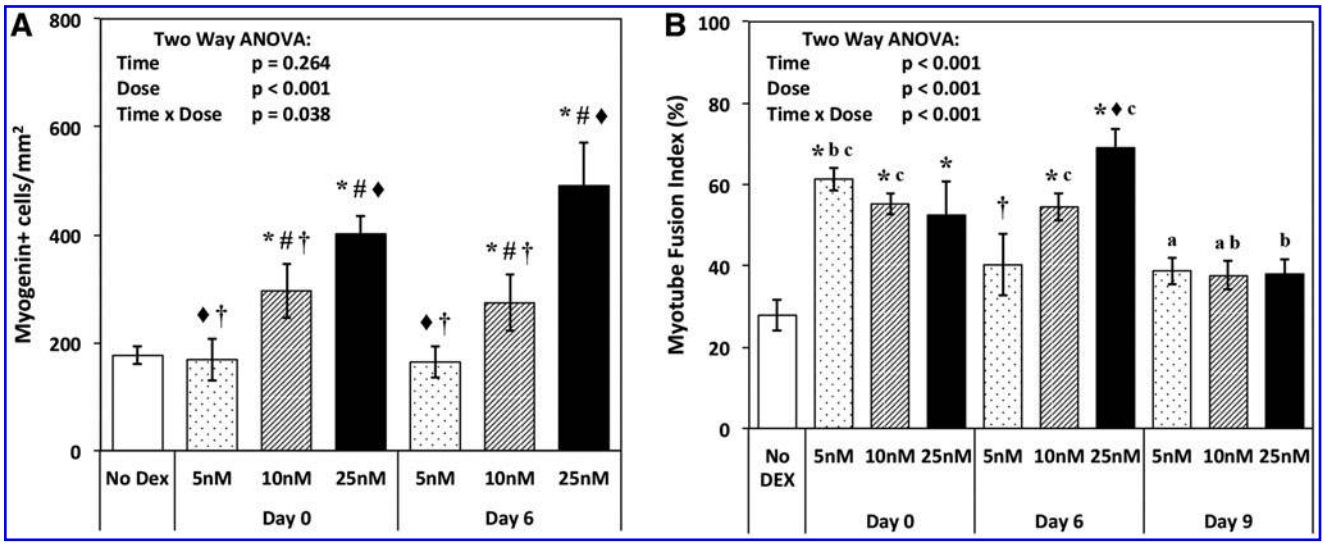

FIG. 3. DEX effects on myogenic differentiation. **(A)** ICC analysis for myogenin on day 7 indicated terminal differentiation of myoblasts into myotubes. Following two-way ANOVA, a dose-dependent increase in myogenin-positive cell density was observed in response to DEX ($p < 0.001$), independent of the timing of addition. **(B)** Myotube fusion index, calculated from desmin and DAPI staining on day 11, quantified the number of nuclei associated with a myotube as a percentage of total nuclei. Two-way ANOVA indicated a significant effect of both DEX dose and timing ($p < 0.001$ for both). When averaged across the three timing groups, all three DEX concentrations yielded significantly increased myotube fusion relative to No DEX controls ($p = 0.002$ for 5 nM, $p > 0.001$ for 10 and 25 nM). Similarly, fusion index increased significantly with DEX addition on day 0 and day 6 ($p = 0.015$ and 0.008, respectively). Error bars indicate mean ± standard error. *Indicates statistical difference from No DEX controls, [#]from 5 nM in the same DEX timing group, [◆]from 10 nM in the same timing group, [†]from 25 nM in the same timing group, [a]from day 0 at the same DEX dose, [b]from day 6 at the same DEX dose, and [c]from day 9 at the same DEX dose.

increased the number cells expressing myogenin ($p = 0.001$), and 25 nM DEX led to even greater increases ($p < 0.001$). Ultimately, treatment with 25 nM DEX beginning on day 6 yielded the highest density of myogenin$^+$ cells, ~2.8 times greater than untreated controls.

Myotube fusion index was measured to assess the ability of myoblasts to terminally differentiate and form a network of myotubes in the presence of DEX. Expression of desmin, a protein specific to muscle cells and a key subunit in intermediate filaments,[17,31] identified fused myotubes, and subsequent analysis of the percentage of nuclei associated with a myotube yielded a myotube fusion index value. Two-way ANOVA indicated that both the dose and timing of DEX addition significantly affected myotube fusion (Fig. 3B). Compared with untreated controls, all three experimental concentrations significantly increased myotube fusion ($p = 0.002$ for 5 nM, $p > 0.001$ for 10 and 25 nM). The effect of time indicates that the early addition of DEX at cell seeding (day 0) or toward the end of the proliferative stage (day 6) significantly increased myotube fusion ($p = 0.015$ and 0.008, respectively), whereas plates treated with DEX during the differentiation stage (day 9) exhibited no difference from controls. Although no difference in myotube fusion was observed between the 5, 10, and 25 nM concentrations when averaged across the three timing groups, focus on the day 6 time point alone revealed a dose-dependent trend, with fusion index increasing with each DEX concentration. This trend included a statistically significant difference between the day 6 DEX concentrations of 5 and 25 nM ($p = 0.007$). Across all experimental groups, addition of 25 nM DEX on day 6 yielded the highest myotube fusion index at 69%, a 250% increase over the No DEX controls. The combined results for myogenin expression and myotube fusion demonstrate that DEX addition increased myogenic differentiation and myotube fusion, with the addition of the highest experimental dose, 25 nM, on day 6 producing the greatest increases.

Further analysis of myotube size and number was performed on day 14, immediately before monolayer delamination. The dose and timing of DEX addition were observed to have significant effects on myotube diameter (Fig. 4B). In response to the experimental DEX concentrations, a significant dose-dependent increase in myotube diameter was observed, resulting in myotubes 1.23, 1.34, and 1.41 times larger than No DEX controls following addition of 5, 10, and 25 nM DEX, respectively ($p = 0.001$ for 5 nM, $p < 0.001$ for 10 and 25 nM). Additionally, in plates receiving DEX at the two early time points, day 0 and day 6, myotube diameters increased significantly relative to untreated controls ($p < 0.001$ for both days). Plates subsequently treated with DEX on day 9 showed no difference in myotube diameter from controls. Day 6 addition of 10 and 25 nM DEX produced the largest myotubes, with average diameters of 14.8 and 16.1 μm, respectively. Myotube diameters for both doses were significantly greater than control myotubes, which had an average diameter of 9.8 μm ($p < 0.001$ for both doses). The effects of the timing of DEX addition on the overall density of the myotube network were also evident. Administration of DEX on day 6 improved myotube density significantly ($p = 0.008$), while addition of DEX on day 0 and day 9 exhibited no significant differences from untreated controls. Similarly, no significant differences were observed when examining the influence of the three DEX

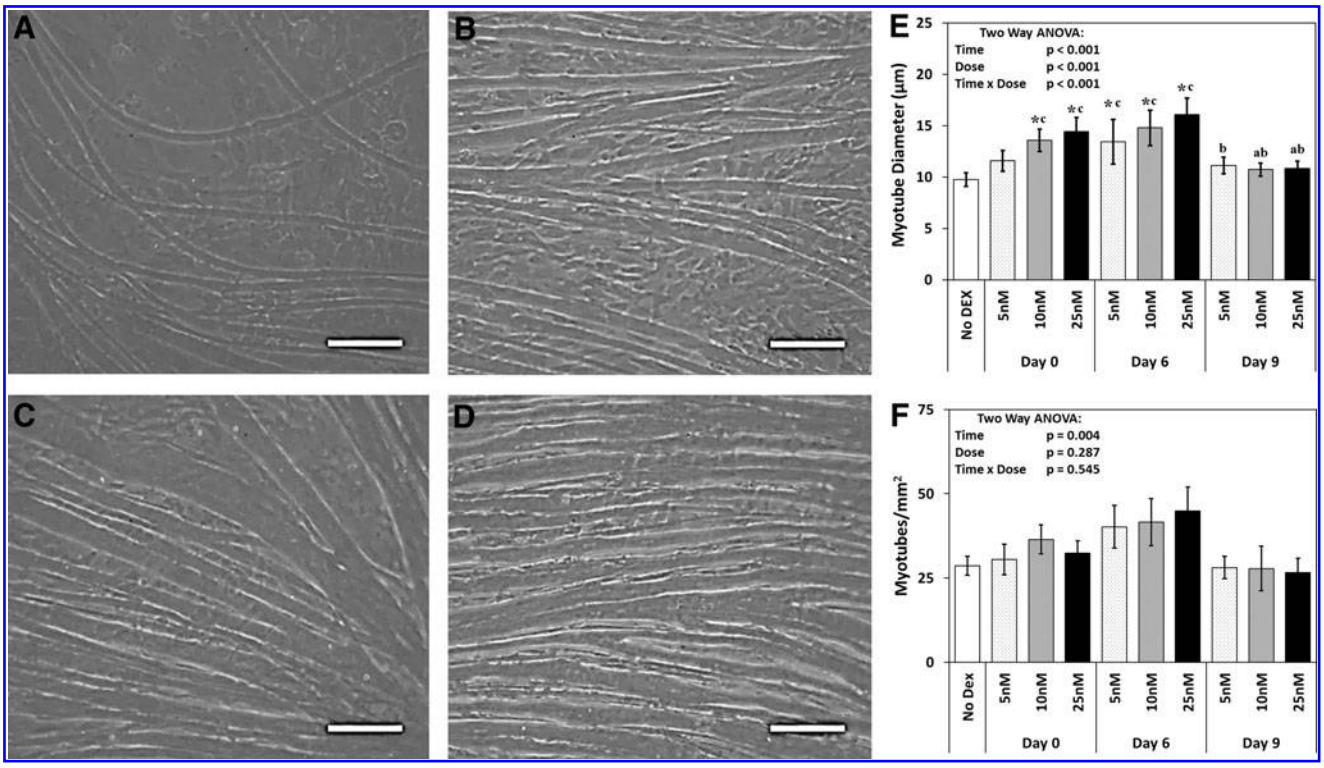

FIG. 4. DEX effects on myotube growth. Monolayers were observed just before delamination on day 14. Representative images are shown above for **(A)** No DEX, **(B)** day 6 (5 nM), **(C)** day 6 (10 nM), and **(D)** day 6 (25 nM). Images from the day 6 timing group were chosen because this time point demonstrated the significant effects of DEX addition detailed below. All images were analyzed for **(E)** myotube diameter and **(F)** myotube density. The effects of DEX dose and timing on myotube size were both evident from two-way ANOVA ($p < 0.001$ for both). *Post hoc* analysis demonstrated significant increases in myotube diameter in response to all three DEX concentrations ($p = 0.001$ for 5 nM, $p < 0.001$ for 10 and 25 nM). Similarly, day 0 and day 6 DEX addition led to significantly increased myotube diameters relative to untreated controls ($p < 0.001$ for both days). When examining myotube density, the timing of DEX addition had a significant effect ($p = 0.004$). Specifically, the number of myotubes increased significantly with DEX addition on day 6 in comparison to No DEX controls ($p = 0.008$), but day 0 and day 9 addition resulted in no significant difference. Scale bars = 100 μm. Error bars indicate mean ± standard error. *Indicates statistical difference from No DEX controls, [a]from day 0 at the same DEX dose, [b]from day 6 at the same dose, and [c]from day 9 at the same dose.

doses on myotube density. Together, the myotube size and density data indicate that the addition of DEX on day 6 leads to a more robust network of larger myotubes, which may be preferable for engineering skeletal muscle.

Structural and functional maturation of 3D SMUs with DEX addition

The influence of DEX on the overall structure and function of engineered SMUs was also observed during delamination and in the final 3D form. Immunocytochemical analysis of α-actinin (Fig. 5A, B) demonstrated improved maturation of myotubes in the delaminating monolayer following addition of all three DEX concentrations. Plates receiving DEX on day 0 and day 6 exhibited advanced sarcomeric structure within highly aligned myofibrils in the confluent monolayers. This development of sarcomeric structure was not observed in control muscle cultures or plates receiving DEX during the differentiation stage on day 9. Similarly, administration of DEX led to improved structural maturation in the fully formed 3D SMUs. Electron micrographs of a SMU receiving 10 nM DEX on day 6 suggested an increase on the density of aligned collagen fibers at the junctions of each myofiber, indicating a more developed ECM than the No DEX SMU (Fig. 5C, D). Furthermore, following 10 nM DEX administration on day 6, the resulting SMU demonstrated development of aligned myofilaments and maturing Z-lines, similar to the organization of parallel sarcomeres in adult skeletal muscle (Fig. 5E, F). Aligned myofilaments were evident in untreated control SMUs, but few developing sarcomeric structures were observed.

This improved structural maturation translated to increased function, as assessed by contractile force production in the 3D SMUs. The maximum isometric tetanic forces produced by engineered SMUs are displayed in Figure 6A, and two-way ANOVA indicated both DEX timing and dose significantly affected SMU function. When averaging the values across all experimental concentrations to study timing effects, administration of DEX on day 0 and day 6 both led to a significant, twofold increase in force production ($p = 0.016$ for day 0, $p = 0.018$ for day 6). Addition of DEX on day 9 led to a 20% decrease in force production compared to No DEX controls. Surprisingly, however, when examining the effects of DEX dosage, only addition of 10 nM DEX produced a significant improvement in function, represented by a fivefold increase in isometric force production relative to No DEX controls

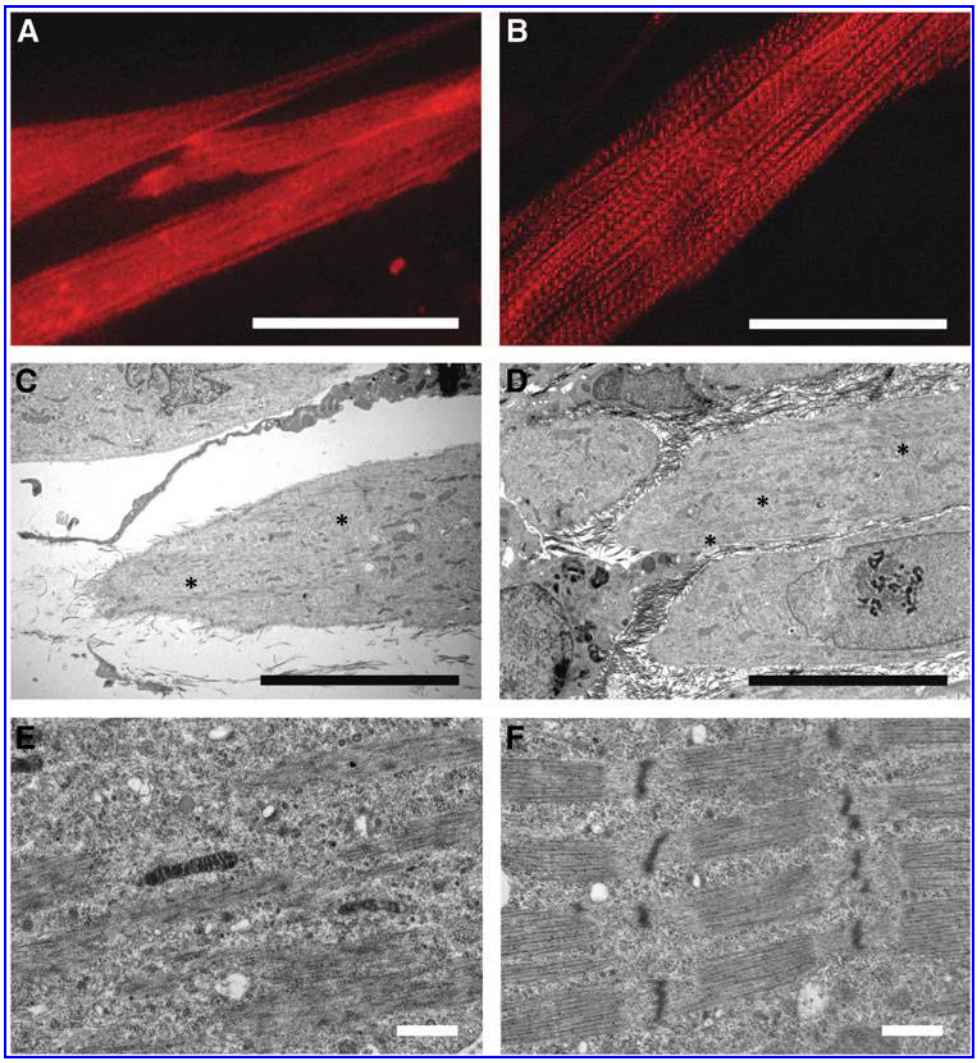

FIG. 5. SMU structural maturation with DEX addition. Representative images of muscle monolayers **(A)** without DEX and **(B)** following DEX addition (day 0, 10 nM). These images show α-actinin in muscle monolayers 10 days post-seeding. Formation of advanced sarcomeric structure and aligned myofibrils was evident in plates receiving DEX on either day 0 or day 6 in all three experimental concentrations. Transmission electron micrographs of longitudinal sections of SMUs following formation of a 3D construct, **(C, E)** without DEX administration and **(D, F)** following day 6 addition of 10 nM DEX, corroborate the positive effects of DEX on structural maturation during SMU fabrication. Both No DEX and day 6, 10 nM DEX images show developing extracellular matrix at myofiber junctions, but greatly increased density and alignment of collagen fibers is evident following DEX addition. Similarly, both SMUs contain myofibers with highly aligned myofilaments, indicated by *asterisks* in **(C, D)**. However, the formation of organized Z-lines indicative of developing sarcomeric structure was observed to a much greater extent in SMUs receiving DEX administration, evident in **(E, F)**. Scale bars in **(A, B)** 50 μm, **(C, D)** 4 μm, **(E, F)** 600 nm.

($p = 0.004$). SMUs receiving 5 nM DEX showed no increase relative to control SMUs, whereas addition of 25 nM DEX significantly decreased force production ($p = 0.024$). Overall, optimal force production was observed in SMUs receiving 10 nM DEX on day 0 and day 6, with average isometric tetanic forces of 256.5 and 253.6 μN, respectively.

Additionally, administration of DEX may have affected the development and maintenance of passive tension in the maturing muscle monolayers, and eventually in the SMUs fabricated from the monolayers. This passive tension effect was quantitatively observed in the timing of delamination of the developing monolayers. Rather than rolling up on day 14 as is typical in our SMU fabrication protocol, plates treated with DEX remained in monolayer form ~20% longer, regardless of the dosage administered. Plates receiving DEX rolled up, on average, on day 17, and manual manipulation was occasionally necessary to assist this process. Following delamination, passive tension development in the newly formed SMUs was measured during assessment of contractile force production 24 h post roll-up. Two-way ANOVA indicated a significant effect of both DEX timing and dose on passive tension (Fig. 6B). Further analysis showed that addition of DEX addition significantly decreased passive tension in fabricated SMUs ($p < 0.001$ for days 0 and 6, $p = 0.006$ for day 9, $p < 0.001$ for 5 nM, $p = 0.003$ for 10 nM, and $p = 0.002$ for 25 nM), regardless of the timing or dose of DEX administration.

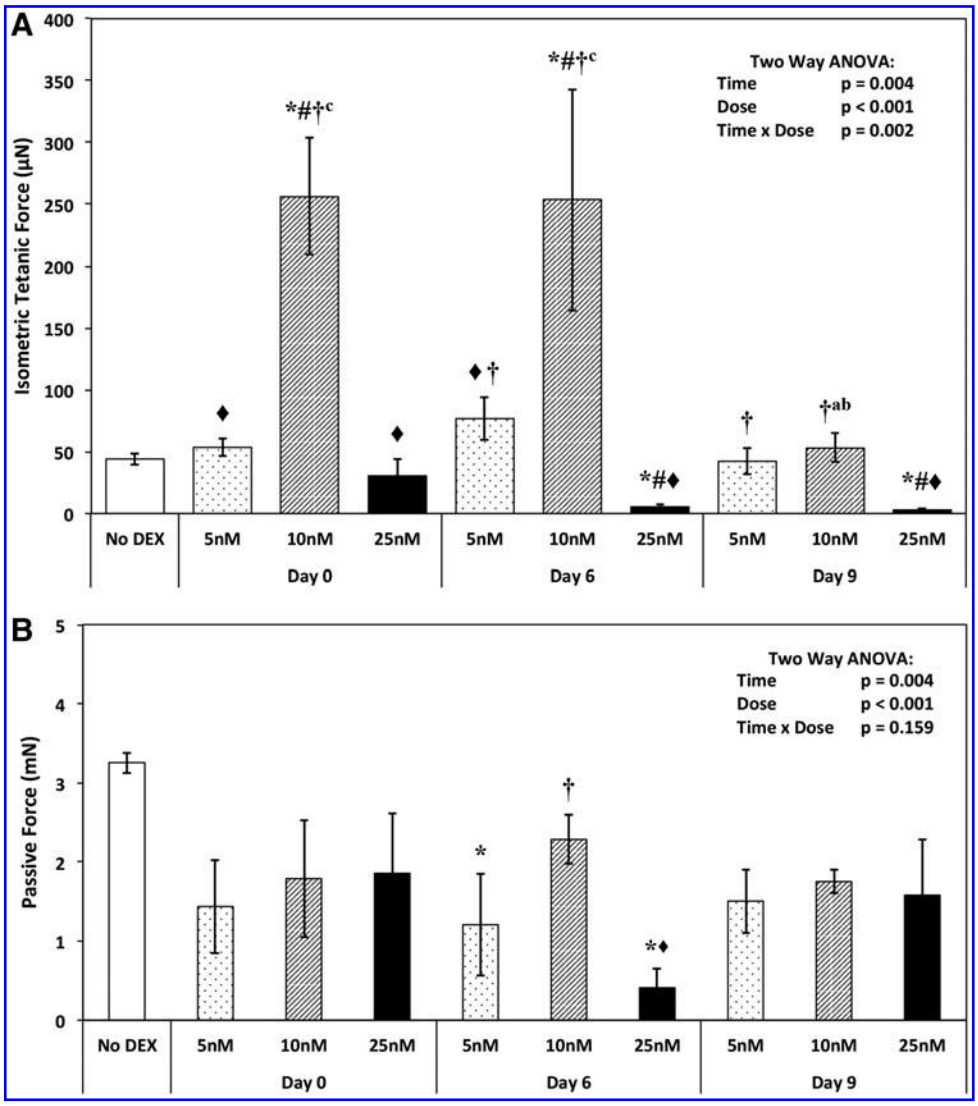

FIG. 6. SMU functional maturation with DEX addition. **(A)** Analysis of the functional measures of isometric tetanic force in 3D SMUs indicated a significant effect of both DEX dose and timing ($p < 0.001$ for dose, $p = 0.004$ for timing). One can conclude that the addition of 10 nM DEX is optimal for SMU fabrication, since this concentration produced a significant, fivefold increase in force production relative to untreated controls ($p = 0.004$). Additionally, day 0 and day 6 administration of DEX both led to a significant, twofold increase in force production ($p = 0.016$ for day 0, $p = 0.018$ for day 6), whereas day 9 DEX addition actually yielded a 20% decrease in force production compared to No DEX controls. **(B)** Examination of passive force generation in fabricated SMUs also showed a significant effect of DEX timing and dose ($p = 0.004$ for timing, $p < 0.001$ for dose). Further analysis indicated that DEX treatment led to significant decreases compared with No DEX controls regardless of DEX timing or concentration ($p < 0.001$ for days 0 and 6, $p = 0.006$ for day 9, $p < 0.001$ for 5 nM, $p = 0.003$ for 10 nM, $p = 0.002$ for 25 nM). Error bars indicate mean ± standard error. *Indicates statistical difference from No DEX controls, [#]from 5 nM in the same DEX timing group, [◆] from 10 nM in the same DEX timing group, [†]from 25 nM in the same DEX timing group, [a]from day 0 at the same DEX dose, [b]from day 6 at the same dose, and [c]from day 9 at the same dose.

Discussion

The overall effects of DEX during the SMU fabrication process can be divided into distinct proliferation, differentiation, and maturation phases. The addition of DEX before myocyte differentiation led to improved myogenic proliferation and suppression of non-myogenic proliferation, indicated by increased $MyoD^+$ cell density and decreased $FSP1^+$ cell density. In addition, administration of 10 and 25 nM DEX at the beginning of proliferation (day 0) or 1 day before the transition from proliferation to differentiation (day 6) yielded increased myoblast fusion, resulting in a dense network of larger myotubes in the subsequent differentiation phase. Similarly, addition of DEX during the proliferative stage on either day 0 or day 6 resulted in the greatest structural maturation of the delaminating monolayers and the resulting fully formed 3D SMUs, characterized by the presence of advanced sarcomeric structure within highly aligned myofibrils. Ultimately, administration of 10 nM DEX during proliferation on either day 0 or day 6 yielded optimal force production in fabricated SMUs.

Although administration of 25 nM DEX improved myogenic proliferation and differentiation, force production in these SMUs actually decreased compared with No DEX controls. Several factors potentially explain the ultimate decrease in the contractile function associated with addition of 25 nM DEX. As described above, supplementation with DEX led to decreased non-myogenic proliferation and increased myogenesis, concomitant with decreased passive tension. ECM is essential to SMU fabrication, both for generation of the passive tension promoting delamination and for structural support of the contractile components of the SMU. Although TEM images indicated increased collagen deposition and alignment following DEX treatment (Fig. 5C, D), this increase in collagen content did not translate to a stiffer ECM, as evidenced by the decrease in passive tension values. It is possible that a more compliant ECM was beneficial to myogenesis. Since plates receiving 25 nM DEX exhibited the largest myotubes in the highest density, however, additional ECM would be required to support these robust muscle networks, and it is possible that the ECM present in the 25 nM plates was insufficient to transmit force along the SMUs.

Another potential explanation was the formation of blebs on the periphery of several myotubes accompanying myoblast fusion. This blebbing typically began shortly after the switch from MGM to MDM on day 7 and became more pronounced during differentiation. Upon gross examination, these blebs were increasingly prevalent at the 25 nM DEX dosage. Blebbing has been identified as a potential biomarker of cell injury that can occur in myotubes in response to toxic agents or hypotonic osmotic shock.[32] Based on the current understanding of the action of DEX *in vivo*,[20,22] namely acting as a potential agent for the induction of skeletal muscle atrophy, it may be possible to draw a connection between DEX addition and myotube membrane damage and blebbing. Further analysis is necessary to determine whether membrane blebbing, an inhibition of ECM formation, or some additional unexpected cause, resulted in the decrease in force production accompanying 25 nM DEX addition.

In conclusion, this experiment demonstrates that addition of DEX to isolated muscle satellite cells in culture can improve functional and structural characteristics of our tissue engineered skeletal muscle when administered at optimal doses and timings. Addition of DEX before induction of differentiation improved myogenic proliferation of muscle satellite cells, which subsequently led to increased myogenic differentiation and myotube fusion. The benefits of the administration of DEX during proliferation were further evident during the SMU maturation phase, as characterized by formation of advanced sarcomeric structure and increased contractile function observed in the fully formed 3D SMU. The most promising improvements in SMU function were achieved with the addition of 10 nM DEX on either day 0 or day 6. In addition to increased myogenic differentiation and myotube fusion, SMUs exposed to this concentration exhibited advanced structural development of sarcomeric structure and a fivefold increase in force production. Thus, the utilization of DEX in our existing tissue engineering model presents a blueprint for advancing tissue engineering of skeletal muscle.

Acknowledgments

The authors would like to acknowledge the support of the NIH R56 grant: 2-R56-AR-054778-06-A1 and the Microfluidics in Biomedical Sciences Training Program: NIH NIBIB T32 EB005582.

Disclosure Statement

No competing financial interests exist.

References

1. Koning, M., Harmsen, M.C., van Luyn, M.J.A., and Werker, P.M.N. Current opportunities and challenges in skeletal muscle tissue engineering. J Tissue Eng Regen Med **3,** 407, 2009.
2. Bach, A.D., Stern-Straeter, J., Beier, J.P., Bannasch, H., and Stark, G.B. Engineering of muscle tissue. Clin Plastic Surg **30,** 589, 2003.
3. Lee, P.H.U., and Vandenburgh, H.H. Skeletal muscle atrophy in bioengineered skeletal muscle: a new model system. Tissue Eng Part A **19,** 2147, 2013.
4. Sakar, M.S., Neal, D., Boudou, T., Borochin, M.A., Li, Y., Weiss, R., Kamm, R.D., Chen, C.S., and Asada, H.H. Formation and optogenetic control of engineered 3D skeletal muscle bioactuators. Lab Chip **12,** 4976, 2012.
5. Neal, D., Sakar, M.S., Ong, L.S., and Asada, H.H. Formation of elongated fascicle-inspired 3D tissues consisting of high-density, aligned cells using sacrificial outer molding. Lab Chip **14,** 1907, 2014.
6. Juhas, M., Engelmayr, G.C., Fontanella, A.N., Palmer, G.M., and Bursac, N. Biomimetic engineered muscle with capacity for vascular integration and functional maturation in vivo. Proc Natl Acad Sci U S A **111,** 5508, 2014.
7. Williams, M.L., Kostrominova, T.Y., Arruda, E.M., and Larkin, L.M. Effect of implantation on engineered skeletal muscle constructs. J Tissue Eng Regen Med **7,** 434, 2013.
8. Corona, B.T., Ward, C.L., Baker, H.B., Walters, T.J., and Christ, G.J. Implantation of in vitro tissue engineered muscle repair constructs and bladder acellular matrices partially restore in vivo skeletal muscle function in a rat model of volumetric muscle loss injury. Tissue Eng Part A **20,** 705, 2014.
9. VanDusen, K.W., Syverud, B.C., Williams, M.L., Lee, J.D., and Larkin, L.M. Engineered skeletal muscle units for repair of volumetric muscle loss in the tibialis anterior muscle of a rat. Tissue Eng Part A **20,** 2920, 2014.
10. Martin, N.R.W., Passey, S.L., Player, D.J., Khodabukus, A., Ferguson, R.A., Sharples, A.P., Mudera, V., Baar, K., and Lewis, M.P. Factors affecting the structure and maturation of human tissue engineered skeletal muscle. Biomaterials **34,** 5759, 2013.
11. Dennis, R., Smith, B., Philp, A., Donnelly, K., and Baar, K. Bioreactors for guiding muscle tissue growth and development. Adv Biochem Eng Biotechnol **112,** 39, 2009.
12. Sicari, B.M., Rubin, J.P., Dearth, C.L., Wolf, M.T., Ambrosio, F., Boninger, M., Turner, N.J., Weber, D.J., Simpson, T.W., Wyse, A., Brown, E.H.P., Dziki, J.L., Fisher, L.E., Brown, S., and Badylak, S.F. An acellular biologic scaffold promotes skeletal muscle formation in mice and humans with volumetric muscle loss. Sci Transl Med **6,** 1, 2014.
13. Wu, X., Corona, B.T., Chen, X., and Walters, T.J. A standardized rat model of volumetric muscle loss injury for

the development of tissue engineering therapies. Biores Open Access **1,** 280, 2012.
14. Lam, M.T., Huang, Y., Birla, R.K., and Takayama, S. Microfeature guided skeletal muscle tissue engineering for highly organized 3-dimensional free-standing constructs. Biomaterials **30,** 1150, 2009.
15. Carosio, S., Barberi, L., Rizzuto, E., Nicoletti, C., Del Prete, Z., and Musarò, A. Generation of eX ivo-vascularized Muscle Engineered Tissue (X-MET). Sci Rep **3,** 1420, 2013.
16. Clegg, C.H., Linkhart, T.A., Olwin, B.B., and Hauschka, S.D. Growth factor control of skeletal muscle differentiation: commitment to terminal differentiation occurs in G1 phase and is repressed by fibroblast growth factor. J Cell Biol **105,** 949, 1987.
17. Allen, R.E., Temm-Grove, C.J., Sheehan, S.M., and Rice, G. Skeletal muscle satellite cell cultures. Methods Cell Biol **52,** 155, 1997.
18. Doumit, M.E., and Merkel, R.A. Conditions for isolation and culture of porcine myogenic satellite cells. Tissue Cell **24,** 253, 1992.
19. Zimmerman, H.J. Hepatotoxicity: The Adverse Effects of Drugs and Other Chemicals on the Liver. Philadelphia: Lippincott Williams & Wilkins, 1999.
20. Inder, W.J., Jang, C., Obeyesekere, V.R., and Alford, F.P. Dexamethasone administration inhibits skeletal muscle expression of the androgen receptor and IGF-1 implications for steroid-induced myopathy. Clin Endocrinol (Oxf) **73,** 126, 2010.
21. Dracott, B.N., and Smith, C.E. Hydrocortisone and the antibody response in mice. II. Correlations between serum and antibody and PFC in thymus, spleen, marrow and lymph nodes. Immunology **38,** 437, 1979.
22. Qin, J., Du, R., Yang, Y., Zhang, H., Li, Q., Liu, L., Guan, H., Hou, J., and An, X. Dexamethasone-induced skeletal muscle atrophy was associated with upregulation of myostatin promoter activity. Res Vet Sci **94,** 84, 2013.
23. Belanto, J.J., Diaz-Perez, S.V., Magyar, C.E., Maxwell, M.M., Yilmaz, Y., Topp, K., Boso, G., Jamieson, C.H., Jamieson, C.A.M., and Cacalano, N.A. Dexamethasone induces dysferlin in myoblasts and enhances their myogenic differentiation. Neuromuscul Disord **20,** 111, 2010.
24. Desler, M.M., Jones, S.J., Smith, C.W., and Woods, T.L. Effects of dexamethasone and anabolic agents on proliferation and protein synthesis and degradation in C2C12 myogenic cells. J Anim Sci **74,** 1265, 1996.
25. Committee for the Update of the Guide for the Care and Use of Laboratory Animals. Guide for the Care and use of Laboratory Animals: Eighth Edition. Washington (DC): National Academies Press, 2010.
26. Larkin, L.M., Calve, S., Kostrominova, T.Y., and Arruda, E.M. Structure and functional evaluation of tendon-skeletal muscle constructs engineered in vitro. Tissue Eng **12,** 3149, 2006.
27. Larkin, L.M., Kuzon, W.M., Jr., Supiano, M.A., Galecki, A., and Halter, J.B. Effect of age and neurovascular grafting on the mechanical function of medial gastrocnemius muscles of Fischer 344 rats. J Gerontol A Biol Sci Med Sci **53,** B252, 1998.
28. Dennis, R.G., and Kosnik II, P.E. Excitability and isometric contractile properties of mammalian skeletal muscle constructs engineered in vitro. In Vitro Cell Dev Biol Anim **36,** 327, 2000.
29. Blitterswijk, C.V., Rouwkema, J., Mulligan, R.C., Langer, R., Garfein, E.S., D'Amore, P.A., Marini, R., Kohane, D.S., Macdonald, M., Darland, D.C., and Levenberg, S. Engineering vascularized skeletal muscle tissue. Nat Biotechnol **23,** 879, 2005.
30. McFarland, D.C., Pesall, J.E., Coy, C.S., and Velleman, S.G. Effects of 17ß-estradiol on turkey myogenic satellite cell proliferation, differentiation, and expression of glypican-1, MyoD and myogenin. Comp Biochem Physiol A Mol Integr Physiol **164,** 565, 2013.
31. Jacquemin, V., Furling, D., Bigot, A., Butler-Browne, G.S., and Mouly, V. IGF-1 induces human myotube hypertrophy by increasing cell recruitment. Exp Cell Res **299,** 148, 2004.
32. Wang, B., Yang, Z., Brisson, B.K., Feng, H., Zhang, Z., Welch, E.M., Peltz, S.W., Barton, E.R., Brown Jr., R.H., and Sweeney, H.L. Membrane blebbing as an assessment of functional rescue of dysferlin-deficient human myotubes via nonsense suppression. J Appl Physiol **109,** 901, 2010.

Address correspondence to:
Brian C. Syverud, MS
Department of Biomedical Engineering
University of Michigan
2328 BSRB
109 Zina Pitcher Place
Ann Arbor, MI 48109-2200

E-mail: bsyverud@umich.edu

Received: December 7, 2015
Accepted: January 1, 2016
Online Publication Date: February 19, 2016

This article has been cited by:

1. Brittany L. Rodriguez, Lisa M. Larkin. Functional three-dimensional scaffolds for skeletal muscle tissue engineering 279-304. [Crossref]
2. R. Witt, A. Weigand, A. M. Boos, A. Cai, D. Dippold, A. R. Boccaccini, D. W. Schubert, M. Hardt, C. Lange, A. Arkudas, R. E. Horch, J. P. Beier. 2017. Mesenchymal stem cells and myoblast differentiation under HGF and IGF-1 stimulation for 3D skeletal muscle tissue engineering. *BMC Cell Biology* **18**:1. . [Crossref]
3. Syverud Brian C., Lin Eric, Nagrath Sunitha, Larkin Lisa M.. Label-Free, High-Throughput Purification of Satellite Cells Using Microfluidic Inertial Separation. *Tissue Engineering Part C: Methods*, ahead of print. [Abstract] [Full Text HTML] [Full Text PDF] [Full Text PDF with Links]
4. Syverud Brian C., Mycek Mary-Ann, Larkin Lisa M.. 2017. Quantitative, Label-Free Evaluation of Tissue-Engineered Skeletal Muscle Through Multiphoton Microscopy. *Tissue Engineering Part C: Methods* **23**:10, 616-626. [Abstract] [Full Text HTML] [Full Text PDF] [Full Text PDF with Links]
5. Neil R.W. Martin, Mark C. Turner, Robert Farrington, Darren J. Player, Mark P. Lewis. 2017. Leucine elicits myotube hypertrophy and enhances maximal contractile force in tissue engineered skeletal muscle in vitro. *Journal of Cellular Physiology* **232**:10, 2788-2797. [Crossref]
6. Mr. Brian C Syverud, Mr. Eric Lin, Dr. Sunitha Nagrath, Dr. Lisa Marie Larkin. Label-Free, High-Throughput Purification of Satellite Cells Using Microfluidic Inertial Separation. *Tissue Engineering Part C: Methods* **0**:ja. . [Abstract] [Full Text PDF] [Full Text PDF with Links]